PHYSICAL REVIEW D **94,** 055007 (2016)

Seesaw scale discrete dark matter and two-zero texture Majorana neutrino mass matrices

J. M. Lamprea* and E. Peinado†

Instituto de Física, Universidad Nacional Autónoma de México, A.P. 20-364, Ciudad de México 01000, México

(Received 14 March 2016; published 8 September 2016)

In this paper we present a scenario where the stability of dark matter and the phenomenology of neutrinos are related by the spontaneous breaking of a non-Abelian flavor symmetry (A_4). In this scenario the breaking is done at the seesaw scale, in such a way that what remains of the flavor symmetry is a Z_2 symmetry, which stabilizes the dark matter. We have proposed two models based on this idea, for which we have calculated their neutrino mass matrices achieving two-zero texture in both cases. Accordingly, we have updated this two-zero texture phenomenology finding an interesting correlation between the reactor mixing angle and the sum of the light neutrino masses. We also have a correlation between the lightest neutrino mass and the neutrinoless double beta decay effective mass, obtaining a lower bound for the effective mass within the region of the nearly future experimental sensitivities.

DOI: 10.1103/PhysRevD.94.055007

I. INTRODUCTION

Neutrino masses, the existence of dark matter (DM), and the baryon asymmetry in the Universe (BAU) are the most important evidences of physics beyond the Standard Model (SM). Here, we propose that the same symmetry explaining neutrino mixing angles is also responsible for the dark matter stability in the context of the discrete dark matter (DDM) mechanism [1]. Under certain conditions, it would be possible also to account for the BAU via leptogenesis. The DDM is based upon the fact that the breaking of a discrete non-Abelian flavor symmetry into one of its subgroups by means of the electroweak symmetry breaking mechanism,[1] accounts for the neutrino masses and mixing pattern and for the dark matter stability.

In the original model [1], the group of even permutation of four objects, A_4, was considered as the flavor symmetry.[2] A_4 contains one tridimensional irreducible representation, 3, and three one-dimensional irreducible representations, $\mathbf{1}$, $\mathbf{1}'$, and $\mathbf{1}''$, whose algebra can be reviewed the Appendix, see, for instance, [2–5]. The particle content includes four $SU(2)$ Higgs doublets, three of them transforming as an A_4 triplet $\eta = (\eta_1, \eta_2, \eta_3)$ and the SM Higgs H as the singlet $\mathbf{1}$; four right-handed (RH) neutrinos, three of them in a triplet representation of A_4, $N_T = (N_1, N_2, N_3)$; and a singlet $\mathbf{1}$ of A_4, N_4. The lepton doublets L_i and the right charged leptons l_i transform as the three different singlets under A_4, in such a way that the mass matrix for the charged lepton is diagonal. Breaking the A_4 symmetry into a Z_2 subgroup through the electroweak symmetry breaking provides the stability mechanism for the DM, arising from the Z_2-odd part of the triplet η and at the same time accounts for the neutrino masses and mixing patterns by means of the type I seesaw [6–11]. The predictions for the neutrino sector are an inverse mass hierarchy spectrum with a massless neutrino, $m_{\nu_3} = 0$,[3] and a vanishing reactor neutrino mixing angle, $\theta_{13} = 0$, that nowadays is ruled out by the current experimental data [12–15]. Even though, there is an issue with the reactor mixing angle, the original A_4 model has a quite interesting neutrino and DM phenomenology, as can be seen in [16].

In a subsequent paper, this A_4 model has been modified [17] by adding a fifth RH neutrino N_5 transforming as $\mathbf{1}''$ and changing the representation of N_4 to $\mathbf{1}'$. This new model gives as predictions a normal mass spectrum, a lower bound for the neutrinoless double beta decay effective mass, $|m_{ee}|$, and a nonzero reactor neutrino mixing angle. Nevertheless, even if this mixing angle were nonzero at its maximum value, it is again ruled out by the current experimental data [12].

There are some other works in this direction, where other flavor symmetry groups have been used, for instance, a model based on the dihedral group D_4 where some flavor changing neutral currents are present and constrain the DM sector [18] and a model based on

*jmlamprea@fisica.unam.mx
†epeinado@fisica.unam.mx

[1]It is possible to break the flavor symmetry with flavon field at another scale other than the electroweak, as we discuss later.

[2]The motivation for choosing A_4 as the flavor group is because it is the smallest non-Abelian discrete group with triplet irreducible representation. Therefore, it is possible to have in the same multiplet some inert and active particles after the flavor symmetry breaking and at the same time a reduced number of couplings for these triplets. Later, we see that this reduced number of couplings is the reason why we got correlations between the observables in the neutrino sector.

[3]This is because only two of the RH neutrinos participate in the seesaw mechanism.

the $\Delta(54)$ [19]. Finally, it is worth mentioning that there have been works tackling the problem of the vanishing reactor mixing angle within the A_4 DDM model [20], but in such a case the A_4 symmetry has to be explicitly broken in the scalar potential. For models in which dark matter transforms nontrivially under a non-Abelian flavor symmetry, see, for instance, [21–23].

The paper is organized as follows: In Sec. II we explain our models giving their matter content and derive the neutrino mass matrices. In Sec. III we discuss the phenomenology, and in Sec. IV we draw our conclusions.

II. REACTOR MIXING ANGLE AND THE DDM MECHANISM

We consider two extensions of the model in Ref. [1], hereafter referred as model A and model B, where in addition to the original model matter content, we have added one extra RH neutrino N_5, in a singlet representation of A_4 ($\mathbf{1}'$ or $\mathbf{1}''$), and three real scalar singlets of the SM transforming as a triplet under A_4, $\phi = (\phi_1, \phi_2, \phi_3)$. The relevant particle content and quantum numbers of model A and model B are summarized in Tables I and II, respectively. The N_5 RH neutrino is assigned to the $\mathbf{1}'$ representation of A_4 in model A and to the $\mathbf{1}''$ A_4 representation in model B. The flavon fields, ϕ, acquire a vacuum expectation value around the seesaw scale, such that A_4 is broken into a Z_2 at this scale instead of at the electroweak scale as in the original model. In this way, the flavon fields contribute to the RH neutrino masses.

A. Model A

If we consider the matter content in Table I, the lepton Yukawa Lagrangian is given by[4]

$$\begin{aligned}\mathcal{L}_{\mathrm{Y}}^{(\mathrm{A})} &= y_e L_e l_e^c H + y_\mu L_\mu l_\mu^c H + y_\tau L_\tau l_\tau^c H \\ &+ y_1^\nu L_e [N_T \eta]_1 + y_2^\nu L_\mu [N_T \eta]_{1''} + y_3^\nu L_\tau [N_T \eta]_{1'} \\ &+ y_4^\nu L_e N_4 H + y_5^\nu L_\tau N_5 H + M_1 N_T N_T + M_2 N_4 N_4 \\ &+ y_1^N [N_T \phi]_3 N_T + y_2^N [N_T \phi]_1 N_4 \\ &+ y_3^N [N_T \phi]_{1''} N_5 + \mathrm{H.c.} \end{aligned} \tag{1}$$

where $[a, b]_j$, stands for the product of the two triplets a, b contracted into the j representation of A_4. In this way, H is responsible for quark (considering the quarks as singlet of A_4) and charged lepton masses, the latter automatically diagonal, $M_l = v_h \mathrm{diag}(y_e, y_\mu, y_\tau)$. The Dirac neutrino mass matrix arises from H and η. The flavon fields will contribute to the RH neutrino mass matrix. Once the flavon fields acquire a vev, A_4 will be broken. In order to preserve a Z_2 symmetry, the alignment of the vevs will be of the form

$$\begin{aligned}&\langle H^0 \rangle = v_h \neq 0, \qquad \langle \eta_1^0 \rangle = v_\eta \neq 0, \qquad \langle \eta_{2,3}^0 \rangle = 0, \\ &\langle \phi_1 \rangle = v_\phi \neq 0, \qquad \langle \phi_{2,3} \rangle = 0. \end{aligned} \tag{2}$$

Therefore, (1, 0, 0) is the vacuum alignment for the A_4 scalar triplets, which is a way to break spontaneously A_4 into a Z_2 subgroup, in the A_4 basis where the S generator is diagonal, see the Appendix.

From Eqs. (1) and (2), the Dirac neutrino mass matrix is given by

$$m_{\mathrm{D}}^{(\mathrm{A})} = \begin{pmatrix} y_1^\nu v_\eta & 0 & 0 & y_4^\nu v_h & 0 \\ y_2^\nu v_\eta & 0 & 0 & 0 & 0 \\ y_3^\nu v_\eta & 0 & 0 & 0 & y_5^\nu v_h \end{pmatrix}, \tag{3}$$

and the Majorana neutrino mass matrix is

$$M_{\mathrm{R}} = \begin{pmatrix} M_1 & 0 & 0 & y_2^N v_\phi & y_3^N v_\phi \\ 0 & M_1 & y_1^N v_\phi & 0 & 0 \\ 0 & y_1^N v_\phi & M_1 & 0 & 0 \\ y_2^N v_\phi & 0 & 0 & M_2 & 0 \\ y_3^N v_\phi & 0 & 0 & 0 & 0 \end{pmatrix}. \tag{4}$$

With these mass matrices, the light neutrinos get Majorana masses through the type I seesaw relation, $m_\nu = -m_{\mathrm{D}_{3\times5}} M_{\mathrm{R}_{5\times5}}^{-1} m_{\mathrm{D}_{3\times5}}^{\mathrm{T}}$, taking the form

$$m_\nu^{(\mathrm{A})} \equiv \begin{pmatrix} a & 0 & b \\ 0 & 0 & c \\ b & c & d \end{pmatrix}, \tag{5}$$

where

TABLE I. Summary of the relevant particle content and quantum numbers for model A.

	L_e	L_μ	L_τ	l_e^c	l_μ^c	l_τ^c	N_T	N_4	N_5	H	η	ϕ
SU(2)	2	2	2	1	1	1	1	1	1	2	2	1
A_4	1	$1'$	$1''$	1	$1''$	$1'$	3	1	$1'$	1	3	3

TABLE II. Summary of the relevant particle content and quantum numbers for model B.

	L_e	L_μ	L_τ	l_e^c	l_μ^c	l_τ^c	N_T	N_4	N_5	H	η	ϕ
SU(2)	2	2	2	1	1	1	1	1	1	2	2	1
A_4	1	$1'$	$1''$	1	$1''$	$1'$	3	1	$1''$	1	3	3

[4]The contribution $y_1^N [N_T \phi]_3 N_T$ accounts for the symmetric part of how the two triplets can be contracted, namely $[N_T \phi]_{3_1}$ and $[N_T \phi]_{3_2}$.

$$a=\frac{(y_4^\nu v_h)^2}{M_2},\quad b=\frac{y_1^\nu y_5^\nu v_\eta v_h}{y_3^N v_\phi}-\frac{y_2^N y_4^\nu y_5^\nu v_h^2}{y_3^N M_2},\quad c=\frac{y_2^\nu y_5^\nu v_\eta v_h}{y_3^N v_\phi},$$
$$d=\frac{(y_2^N y_5^\nu v_h)^2}{(y_3^N)^2 M_2}-\frac{(y_5^\nu v_h)^2 M_1}{(y_3^N v_\phi)^2}+2\frac{y_3^\nu y_5^\nu v_\eta v_h}{y_3^N v_\phi}. \quad (6)$$

The mass matrix in Eq. (5) has the form of the B_3 two-zero neutrino mass matrix [24], which phenomenology has been extensively studied in the literature, see, for instance, [24–33]. This matrix is consistent with both neutrino mass hierarchies and can accommodate the experimental value for the reactor mixing angle, θ_{13} [24–33]. The phenomenological implications of this scenario are studied in Sec. III.

B. Model B

The lepton Yukawa Lagrangian for the matter content and assignments of model B, in Table II, is given by

$$\begin{aligned}\mathcal{L}_Y^{(B)} &= y_e L_e l_e^c H + y_\mu L_\mu l_\mu^c H + y_\tau L_\tau l_\tau^c H \\ &+ y_1^\nu L_e [N_T \eta]_1 + y_2^\nu L_\mu [N_T \eta]_{1''} + y_3^\nu L_\tau [N_T \eta]_{1'} \\ &+ y_4^\nu L_e N_4 H + y_5^\nu L_\mu N_5 H + M_1 N_T N_T + M_2 N_4 N_4 \\ &+ y_1^N [N_T \phi]_3 N_T + y_2^N [N_T \phi]_1 N_4 \\ &+ y_3^N [N_T \phi]_{1'} N_5 + \text{H.c.} \quad (7)\end{aligned}$$

As in model A, the mass matrix of the charged leptons is diagonal, due to the flavor symmetry, while the Dirac neutrino mass matrix takes the form

$$m_D^{(B)}=\begin{pmatrix} y_1^\nu v_\eta & 0 & 0 & y_4^\nu v_h & 0 \\ y_2^\nu v_\eta & 0 & 0 & 0 & y_5^\nu v_h \\ y_3^\nu v_\eta & 0 & 0 & 0 & 0 \end{pmatrix}. \quad (8)$$

The Majorana neutrino mass matrix is of the same form as Eq. (4). The light neutrinos mass matrix after the type I seesaw is

$$m_\nu^{(B)} \equiv \begin{pmatrix} a & b & 0 \\ b & d & c \\ 0 & c & 0 \end{pmatrix}, \quad (9)$$

where

$$a=\frac{(y_4^\nu v_h)^2}{M_2},\quad b=\frac{y_1^\nu y_5^\nu v_\eta v_h}{y_3^N v_\phi}-\frac{y_2^N y_4^\nu y_5^\nu v_h^2}{y_3^N M_2},\quad c=\frac{y_3^\nu y_5^\nu v_\eta v_h}{y_3^N v_\phi},$$
$$d=\frac{(y_2^N y_5^\nu v_h)^2}{(y_3^N)^2 M_2}-\frac{(y_5^\nu v_h)^2 M_1}{(y_3^N v_\phi)^2}+2\frac{y_2^\nu y_5^\nu v_\eta v_h}{y_3^N v_\phi}, \quad (10)$$

which correspond, as before, to another two-zero texture flavor neutrino mass matrix, B_4 [24], which also is consistent with both neutrino mass hierarchies and can also accommodate the reactor mixing angle, θ_{13} [24–33].

III. RESULTS

In the previous section, we obtained the two-zero texture neutrino mass matrices B_3 and B_4 for models A and B, respectively. We performed the analysis using four independent constraints, coming from the two complex zeroes, to correlate two of the neutrino mixing parameters: the neutrino masses and mixing angles, the two Majorana phases, and the Dirac CP violating phase.[5] We took the experimental values of the three mixing angles and the two squared mass differences as inputs and numerically scanned within their 3σ regions and determined the regions allowed by two correlated variables of interest. We have used in the analysis the data from three different groups that perform the neutrino global fits [13–15].

In Figs. 1,3, and 5 we show the correlation between the atmospheric mixing angle, $\sin^2\theta_{23}$, and the sum of light neutrino masses, $\sum m_\nu = m_{\nu_1}+m_{\nu_2}+m_{\nu_3}$, for model A on the left panels and model B on the right ones. In these graphics, the allowed 3σ regions in $\sin^2\theta_{23}$ vs. $\sum m_\nu$ for the normal hierarchy (NH) is plotted in magenta and for the inverse hierarchy (IH) in cyan. The 1σ in the atmospheric angle are represented by the horizontal blue and red shaded regions for the inverted and normal mass hierarchy, respectively, and the best fit values correspond to the horizontal blue and red dashed lines for the inverse and normal hierarchies, respectively. In Forero *et al.* [13], they have a local minimum in the atmospheric mixing angle for the IH analysis; that we represent as a red pointed line in Fig. 1. In addition, in the analysis by Capozzi *et al.* [15], they have obtained two different and separated 1σ regions in the atmospheric angle also for the IH; that we show as the double blue shaded horizontal bands in Fig. 3. The gray vertical band represents a disfavored region in the sum of light neutrino masses, $\sum m_\nu < 0.23$ eV, by the Planck Collaboration [34].

From the plots in Figs. 1,3, and 5, it can be seen that in model A both hierarchies have an overlap within the 1σ region for the atmospheric mixing angle, while in model B depending on what data is used the overlap not always exists. For data from Forero *et al.* [13] and Gonzalez-Garcia *et al.* [14], only the NH the atmospheric mixing angle overlaps with the 1σ region (even though for data from [14] it happens for large neutrino masses disfavored by Planck). For data from Capozzi *et al.* [15], only in the IH case there is the 1σ overlap in the second octant for the atmospheric mixing angle. Finally, it is worth mentioning that the NH and IH regions in model A are the same but interchanged in model B.

[5]The method we have used is known and can be reviewed, for instance, in [30,31].

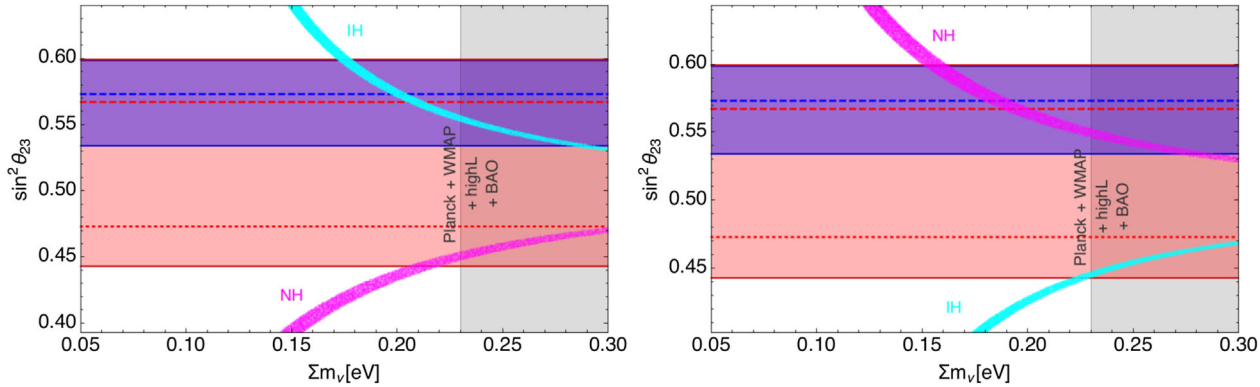

FIG. 1. Correlation between $\sin^2\theta_{23}$ and the sum of the light neutrino masses, $\sum m_\nu$, in model A (B_3) on the left and model B (B_4) on the right, for NH (IH) in magenta (cyan). The horizontal red (blue) shaded region is the 1σ in $\sin^2\theta_{23}$ for NH (IH). The red (blue) horizontal dashed line is the best fit value in NH (IH), and the doted red line is the value of local minimum in NH appearing in the data analysis used. The data was taken from [13]. The vertical gray shaded region is disfavored by the current Planck data [34].

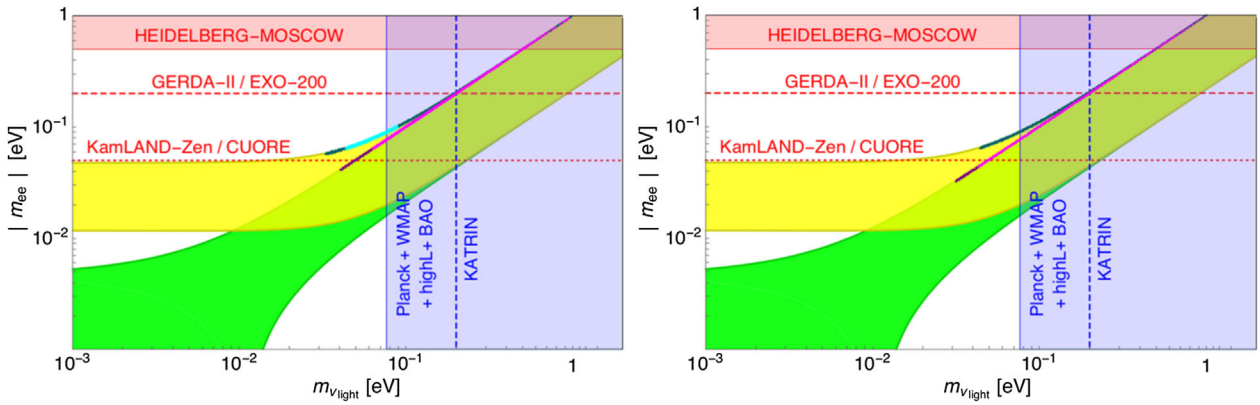

FIG. 2. Effective $0\nu\beta\beta$ parameter $|m_{ee}|$ versus the lightest neutrino mass $m_{\nu_{\text{light}}}$ in model A (B) on the left (right). In both models $m_{\nu_{\text{light}}}$ is $m_1(m_3)$ for NH (IH). The model allowed regions for NH are in magenta (dark magenta) for the 1σ (3σ) atmospheric mixing angle region and for IH in cyan (dark cyan) for the 1σ (3σ) on the atmospheric mixing angle region from [13]. The yellow (green) band correspond to the "flavor-generic" inverse (normal) hierarchy neutrino spectra for 3σ. The horizontal red shaded region is the current experimental limit on $0\nu\beta\beta$, and the red (blue) horizontal (vertical) lines are the forthcoming experimental sensitivity on $|m_{ee}|$ ($m_{\nu_{\text{light}}}$), see [35–40]. The vertical blue shaded regions are disfavored by the current Planck data [34].

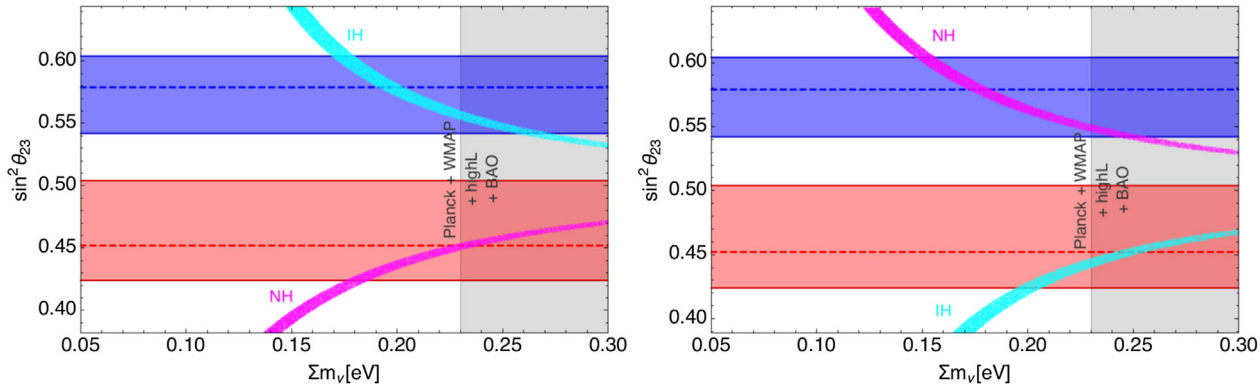

FIG. 3. Correlation between $\sin^2\theta_{23}$ and the sum of the light neutrino masses, $\sum m_\nu$, in model A (B_3) on the left and model B (B_4) on the right, for NH (IH) in magenta (cyan). The red (blue) horizontal dashed line is the best fit value in NH (IH). The data was taken from [14]. The vertical gray shaded region is disfavored by the current Planck data [34].

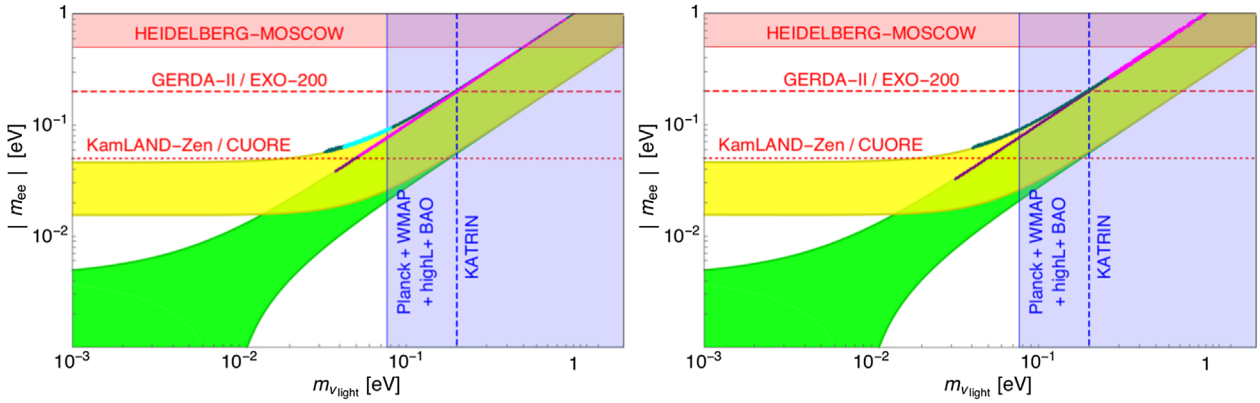

FIG. 4. Effective $0\nu\beta\beta$ parameter $|m_{ee}|$ versus the lightest neutrino mass $m_{\nu_{\rm light}}$ in model A (B) on the (right). In both models $m_{\nu_{\rm light}}$ is $m_1(m_3)$ for NH (IH). The model allowed regions for NH is in magenta (dark magenta) for the 1σ (3σ) for the atmospheric mixing angle and for IH in cyan (dark cyan) for the 1σ (3σ) for the atmospheric mixing angle region from [14]. The horizontal blue (red) shaded region is the 1σ in $\sin^2\theta_{23}$ for IH (NH). The yellow (green) band correspond to the 3σ "flavor-generic" inverse (normal) hierarchy neutrino spectra. The horizontal red shaded region is the current experimental limit on $0\nu\beta\beta$, and the red (blue) horizontal (vertical) lines are the forthcoming experimental sensitivity on $|m_{ee}|$ ($m_{\nu_{\rm light}}$), see [35–40]. The vertical blue shaded regions are disfavored by the current Planck data [34].

The other correlation we obtained in the models is the neutrinoless double beta decay effective mass parameter, $|m_{ee}|$, with the lightest neutrino mass, $m_{\nu_{\rm light}}$, where $m_{\nu_{\rm light}} = m_{\nu_1}$ in the normal hierarchy and $m_{\nu_{\rm light}} = m_{\nu_3}$ in the inverted hierarchy. Figures 2,4, and 6 show $m_{\nu_{\rm light}}$ versus $|m_{ee}|$ for model A (B_3) on the left panels and model B (B_4) on the right ones. The region for the NH within 3σ are in dark magenta and the overlap for the atmospheric mixing angle of 1σ in magenta; similarly, the region corresponding to the IH within 3σ are in dark cyan and within 1σ in cyan. The horizontal red shaded region corresponds the current experimental limit on neutrinoless double beta decay [35]; the red and blue lines are the forthcoming experimental sensitivities on $|m_{ee}|$ [36–39] and $m_{\nu_{\rm light}}$ [40], respectively. The vertical blue shaded region is disfavored by the current Planck data [34]. In the graphics, we also show in yellow and green the bands corresponding to the 3σ "flavor-generic" inverse and normal hierarchy neutrino spectra, respectively.

It can be seen from Figs. 2 and 4 that for model B there is no 1σ overlap between the prediction and the experimental data for the atmospheric mixing angle, and therefore, we only show the data for the 3σ regions in the IH. In Fig. 6, it can be seen that also the results in model B do not overlap with the 1σ region for the NH case, as we mentioned before. The models predict Majorana phases giving a minimal cancelation for the $|m_{ee}|$, as can bee seen in Figs. 2, 4, and 6. The allowed regions for the $|m_{ee}|$ are in the upper lines for NH and IH generic bands. The two-zero textures B_3 and B_4 are sensitive to the value of the atmospheric mixing angle. In the cases in which the atmospheric mixing angle prediction overlaps with the experimental value at 1σ, it translates to a localized region for neutrinoless double beta decay within the near future experimental sensitivity, which is a desirable feature.

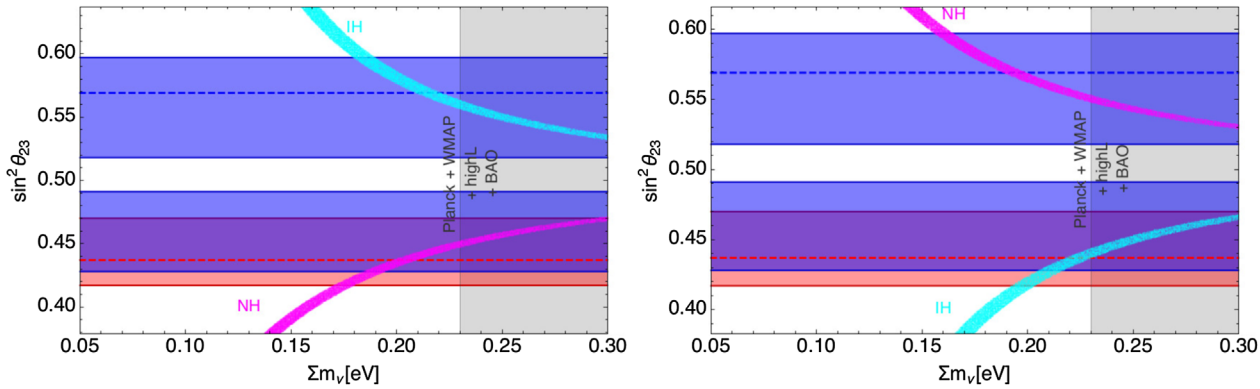

FIG. 5. Correlation between $\sin^2\theta_{23}$ and the sum of the light neutrino masses, $\sum m_\nu$, in model A (B_3) on the and model B (B_4) on the right, for NH (IH) in magenta (cyan). The horizontal red (blue) shaded regions are the 1σ in $\sin^2\theta_{23}$ for NH (IH). The case for IH has two favored 1σ regions according to the data used. The red (blue) horizontal dashed line is the best fit value in NH (IH). The data was taken from [15]. The vertical gray shaded region is disfavored by the current Planck data [34].

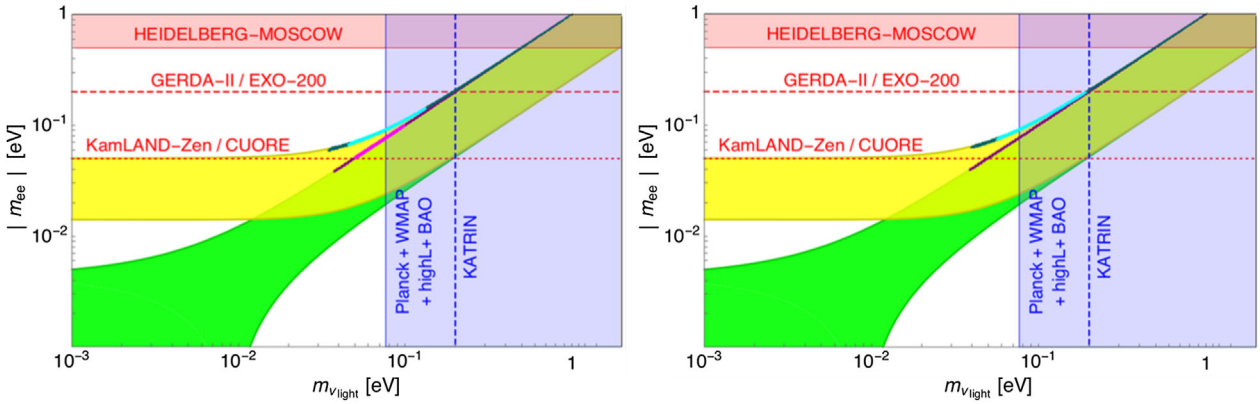

FIG. 6. Effective $0\nu\beta\beta$ parameter $|m_{ee}|$ versus the lightest neutrino mass $m_{\nu_{\text{light}}}$ in model A (B) on the (right). Regions for NH is in magenta (dark magenta) for the 1σ (3σ) atmospheric mixing angle region and the IH in cyan (dark cyan) for the 1σ (3σ) for the atmospheric mixing angle region from [15]. The yellow (green) band correspond to the 3σ "flavor-generic" inverse (normal) hierarchy neutrino spectra. The horizontal red shaded region is the current experimental limit on $0\nu\beta\beta$, and the red (blue) horizontal (vertical) lines are the forthcoming experimental sensitivity on $|m_{ee}|$ ($m_{\nu_{\text{light}}}$), see [35–40]. The vertical blue shaded regions are disfavored by the current Planck data [34].

A better measurement of the atmospheric mixing angle would be crucial for this kind of scenarios.

The dark matter phenomenology arising from the models (A and B) is different from that in the original DDM model, where the limit for large masses ($M_{\text{DM}} > 100$ GeV) was not allowed. The DM phenomenology is similar to the one in the inert Higgs doublet model [41] with two active and two inert Higgses. What can be said about the DM phenomenology is that there is no inconvenience in generating the correct relic abundance even if the mass of the DM candidate is bigger than the mass of the gauge bosons. The limits presented in the minimal dark matter model [42] apply, and for those masses, it annihilates mainly into gauge bosons.

Finally, it is worth mentioning that neutrino phenomenology and the dark matter phenomenology are related by the way A_4 is broken into the Z_2 symmetry. This breaking dictates the pattern of masses and the mixing of the neutrinos, and at the same time, this Z_2 is responsible for the DM stability. This is the connection between DM and neutrinos in the presented models.

IV. CONCLUSIONS

We have constructed two models based on the discrete dark matter mechanism where the non-Abelian A_4 flavor symmetry is spontaneously broken at the seesaw scale into a remanent Z_2. In these models, we have a total of five RH neutrinos. In this case, two RH neutrinos are in the Z_2 odd sector, and the other three RH are even under Z_2. These three RH neutrinos are responsible for giving the light neutrino masses via type I seesaw. Additionally, we have added flavon scalar fields ϕ leading to the A_4 breaking in such a way that we obtained two-zero textures for the light Majorana neutrinos. These textures give rise to rich neutrino phenomenology: The results are in agreement with the experimental data of the reactor mixing angle and accommodate the two possible neutrino mass hierarchies, NH and IH.

Another consequence of the way A_4 is broken, in addition to dictating the neutrino phenomenology, is that these models contain a DM candidate stabilized by the remnant Z_2 symmetry. The DM phenomenology in this case will be different than the original DDM [16], where the limit for large DM masses ($M_{\text{DM}} \gtrsim 100$ GeV) was not allowed, and will be similar to the inert Higgs doublet model [41] with extra scalar fields. A detailed discussion of the DM phenomenology is beyond the scope of the present work and will be presented in a further work [43].

Additionally, we have updated the analysis for the two-zero textures mass matrix obtained for both models B_3 and B_4. We presented the correlation between the atmospheric mixing angle and the sum of the light neutrino masses as well as the lower bounds for neutrinoless double beta decay effective mass parameter; the latter being in the region of sensitivity of the near future experiments. Finally, if the flavon fields acquire vevs at a scale slightly higher than the seesaw scale, the remaining symmetry at the seesaw scale is the Z_2, and this would imply a mixing of the three Z_2 even RH neutrinos, which could be crucial if we want to have a scenario for leptogenesis, since in the A_4 symmetric case this was not possible.[6]

ACKNOWLEDGMENTS

This work has been supported in part by Grants No. PAPIIT IA101516, No. PAPIIT IN111115, No. CONACYT 132059 and SNI. J. M. L. would like to thank CONACYT (México) for financial support.

[6]This is studied somewhere else [43].

APPENDIX: THE A_4 PRODUCT REPRESENTATION

The group A_4 has four irreducible representations: three singlets $\mathbf{1}$, $\mathbf{1}'$, and $\mathbf{1}''$ and one triplet 3 and two generators: S and T following the relations $S^2 = T^3 = (ST)^3 = \mathcal{I}$. The one-dimensional unitary representations are

$$\begin{aligned} \mathbf{1}&: S = 1, \qquad T = 1, \\ \mathbf{1}'&: S = 1, \qquad T = \omega, \\ \mathbf{1}''&: S = 1, \qquad T = \omega^2, \end{aligned} \tag{A1}$$

where $\omega^3 = 1$. In the basis where S is real diagonal,

$$S = \begin{pmatrix} 1 & 0 & 0 \\ 0 & -1 & 0 \\ 0 & 0 & -1 \end{pmatrix} \quad \text{and} \quad T = \begin{pmatrix} 0 & 1 & 0 \\ 0 & 0 & 1 \\ 1 & 0 & 0 \end{pmatrix}. \tag{A2}$$

The product rule for the singlets are

$$\begin{aligned} \mathbf{1} \times \mathbf{1} = \mathbf{1}' \times \mathbf{1}'' = \mathbf{1}, \\ \mathbf{1}' \times \mathbf{1}' = \mathbf{1}'', \\ \mathbf{1}'' \times \mathbf{1}'' = \mathbf{1}', \end{aligned} \tag{A3}$$

and triplet multiplication rules are

$$\begin{aligned} (ab)_1 &= a_1 b_1 + a_2 b_2 + a_3 b_3, \\ (ab)_{1'} &= a_1 b_1 + \omega a_2 b_2 + \omega^2 a_3 b_3, \\ (ab)_{1''} &= a_1 b_1 + \omega^2 a_2 b_2 + \omega a_3 b_3, \\ (ab)_{3_1} &= (a_2 b_3, a_3 b_1, a_1 b_2), \\ (ab)_{3_2} &= (a_3 b_2, a_1 b_3, a_2 b_1), \end{aligned} \tag{A4}$$

where $a = (a_1, a_2, a_3)$ and $b = (b_1, b_2, b_3)$.

[1] M. Hirsch, S. Morisi, E. Peinado, and J. W. F. Valle, Phys. Rev. D **82**, 116003 (2010).
[2] E. Ma and G. Rajasekaran, Phys. Rev. D **64**, 113012 (2001).
[3] K. S. Babu, E. Ma, and J. W. F. Valle, Phys. Lett. B **552**, 207 (2003).
[4] G. Altarelli and F. Feruglio, Nucl. Phys. **B741**, 215 (2006).
[5] G. Altarelli, F. Feruglio, and Y. Lin, Nucl. Phys. **B775**, 31 (2007).
[6] P. Minkowski, Phys. Lett. **67B**, 421 (1977).
[7] T. Yanagida, Conference Proceedings **C7902131**, 95 (1979).
[8] M. Gell-Mann, P. Ramond, and R. Slansky, Conference Proceedings **C790927**, 315 (1979).
[9] S. Glashow, in *Quarks and Leptons* (Cargèse Lectures, Plenum, NY, 1980), p. 687.
[10] J. Schechter and J. W. F. Valle, Phys. Rev. D **22**, 2227 (1980); **25**, 774 (1982).
[11] R. N. Mohapatra and G. Senjanovic, Phys. Rev. D **23**, 165 (1981).
[12] W. Tang (Daya Bay Collaboration), arXiv:1512.00335.
[13] D. V. Forero, M. Tortola, and J. W. F. Valle, Phys. Rev. D **90**, 093006 (2014).
[14] M. C. Gonzalez-Garcia, M. Maltoni, and T. Schwetz, Nucl. Phys. **B908**, 199 (2016).
[15] F. Capozzi, E. Lisi, A. Marrone, D. Montanino, and A. Palazzo, Nucl. Phys. **B908**, 218 (2016).
[16] M. S. Boucenna, M. Hirsch, S. Morisi, E. Peinado, M. Taoso, and J. W. F. Valle, J. High Energy Phys. 05 (2011) 037.
[17] D. Meloni, S. Morisi, and E. Peinado, Phys. Lett. B **697**, 339 (2011).
[18] D. Meloni, S. Morisi, and E. Peinado, Phys. Lett. B **703**, 281 (2011).
[19] M. S. Boucenna, S. Morisi, E. Peinado, Y. Shimizu, and J. W. F. Valle, Phys. Rev. D **86**, 073008 (2012).
[20] Y. Hamada, T. Kobayashi, A. Ogasahara, Y. Omura, F. Takayama, and D. Yasuhara, J. High Energy Phys. 10 (2014) 183.
[21] A. Adulpravitchai, B. Batell, and J. Pradler, Phys. Lett. B **700**, 207 (2011).
[22] I. de Medeiros Varzielas, O. Fischer, and V. Maurer, J. High Energy Phys. 08 (2015) 080.
[23] I. Medeiros Varzielas and O. Fischer, J. High Energy Phys. 01 (2016) 160.
[24] P. H. Frampton, S. L. Glashow, and D. Marfatia, Phys. Lett. B **536**, 79 (2002).
[25] Z. z. Xing, Phys. Lett. B **530**, 159 (2002); **539**, 85 (2002).
[26] P. H. Frampton, M. C. Oh, and T. Yoshikawa, Phys. Rev. D **66**, 033007 (2002).
[27] A. Kageyama, S. Kaneko, N. Shimoyama, and M. Tanimoto, Phys. Lett. B **538**, 96 (2002).
[28] A. Merle and W. Rodejohann, Phys. Rev. D **73**, 073012 (2006).
[29] H. Fritzsch, Z. z. Xing, and S. Zhou, J. High Energy Phys. 09 (2011) 083.
[30] P. O. Ludl, S. Morisi, and E. Peinado, Nucl. Phys. **B857**, 411 (2012).
[31] D. Meloni, A. Meroni, and E. Peinado, Phys. Rev. D **89**, 053009 (2014).
[32] S. Zhou, Chin. Phys. C **40**, 033102 (2016).
[33] T. Kitabayashi and M. Yasuè, Phys. Rev. D **93**, 053012 (2016).
[34] P. A. R. Ade *et al.* (Planck Collaboration), arXiv: 1502.01589.
[35] V. E. Guiseppe *et al.* (Majorana Collaboration), The MAJORANA neutrinoless double-beta decay experiment, in *IEEE Nuclear Science Symposium Conference Record Dresden, Germany, 2008*, http://dx.doi.org/10.1109/NSSMIC.2008.4774740, pp. 1793–1798.

[36] M. Agostini *et al.* (GERDA Collaboration), Phys. Rev. Lett. **111**, 122503 (2013).
[37] J. B. Albert *et al.* (EXO-200 Collaboration), Nature (London) **510**, 229 (2014).
[38] A. Gando *et al.* (KamLAND-Zen Collaboration), Phys. Rev. Lett. **110**, 062502 (2013).
[39] A. Giuliani (CUORE Collaboration), J. Phys. Conf. Ser. **120**, 052051 (2008).
[40] L. Bornschein (KATRIN Collaboration), KATRIN: Direct measurement of neutrino masses in the sub-Ev region, eConf C 030626, FRAP14 (2003).
[41] N. G. Deshpande and E. Ma, Phys. Rev. D **18**, 2574 (1978).
[42] M. Cirelli, N. Fornengo, and A. Strumia, Nucl. Phys. **B753**, 178 (2006).
[43] J. M. Lamprea and E. Peinado (to be published).